

---

# Airflow measurement in passively aerated compost

S. Yu\*, O.G. Clark and J.J. Leonard

*Department of Agricultural, Food, and Nutritional Science, University of Alberta, Edmonton, Alberta T6G 2P5, Canada. \*Email: shouhai@ualberta.ca*

---

Yu, S., Clark, O.G. and Leonard, J.J. 2005. **Airflow measurement in passively aerated compost.** *Canadian Biosystems Engineering/Le génie des biosystèmes au Canada* **47**: 6.39 - 6.45. Adequate aeration is necessary to maintain aerobic conditions in compost. Aeration systems are less expensive in terms of capital investment and operating costs if they are passive (convective) rather than active (forced). The flow and control of air has not been as well studied in passive systems, however, partly because of the difficulty of measuring the diffuse, variable, and sometimes extremely low flow rates of saturated air. In this study, a smoke tracer airflow meter was designed to measure airflow through passively aerated compost. Smoke from fuming sulphuric acid was injected into a straight air exhaust pipe and its passage was detected by two infrared emitter/detectors separated by a known distance. The meter was used to effectively measure the flow of moist exhaust air from a passively aerated, laboratory-scale compost vessel. The smoke tracer device was shown to be superior in this application to ultrasonic, hotwire, or bubble airflow meters. **Keywords:** passive aeration, compost, smoke tracer, airflow measurement.

Une aération adéquate est nécessaire pour maintenir des conditions aérobies dans le compost. Les systèmes d'aération passifs (à convection) plutôt qu'actifs (forcés) coûtent moins chers en termes d'investissement en capital ainsi qu'en frais d'exploitation. Cependant, l'écoulement et la commande d'air n'ont pas été aussi bien étudiés dans les systèmes passifs, en partie due à la difficulté de mesurer l'écoulement diffus, variable, et parfois extrêmement bas d'air saturé. Dans cette étude, un débitmètre d'air détectant la fumée a été conçu pour mesurer l'écoulement d'air provenant du compost aéré passivement. De la vapeur d'acide sulfurique a été injectée dans un tuyau d'échappement d'air et son passage a été détecté par deux paires d'émetteurs/détecteurs infrarouges séparées par une distance connue. Le débitmètre a été utilisé pour mesurer efficacement l'écoulement d'air provenant d'un baril de compost aéré passivement. Le débitmètre détecteur de fumée s'est avéré supérieur dans cette application que les débitmètres ultrasoniques, à fil chaud, ou à bulle de savon. **Mots-clés:** Aération passive, compost, écoulement d'air, mesure, détecteur de fumée.

## INTRODUCTION

Composting is often used in waste management systems to treat organic material because of the high degradation rate, low odour generation, and efficient space utilization that can be achieved. Composting is a biological process that must be kept aerobic in order to realize these advantages. The aeration of compost promotes microbial activity by providing oxygen and removing carbon dioxide, ammonia, and excess moisture and heat (Haug 1993). Resistance to airflow varies with the airflow rate and material properties of the compost (Barrington et al. 2002;

Veeken et al. 2002). In actively aerated systems, this resistance is overcome by a pump which draws or blows air through the compost, while in passively aerated systems the driving force is natural convection (Richard 1993; Fogiel et al. 1999).

Initial capital investment and operation, maintenance, and operator training costs are higher for active aeration systems as compared to passive aeration systems (Haug 1993). Passively aerated systems can provide the same process rate as active aeration systems (Fernandez and Sartaj 1997; Solano et al. 2001), and both types of system can operate all year, even in temperate climates (Lynch and Cherry 1995). The quality of compost produced by passive aeration is "remarkably similar" to the product of an active aeration system (Solano et al. 2001). Passive aeration can therefore be considered suitable not only for small-scale applications, but also as a less expensive alternative to active aeration for large-scale processing (Lynch and Cherry 1995; Rynk 1992).

The primary difference between active and passive aeration systems, aside from cost, is that an active system generates a consistently high airflow rate. The airflow rate in a passive system is generally lower and more variable because it is driven by the heat from microbial activity. When microbial activity is low, at the start of the process for instance, then the airflow rate is also low. This variable flow rate in passive aeration can be advantageous, conserving process heat and driving off less nitrogen from the compost. Passive aeration, as a result, is more energy efficient and has been shown to produce compost that is richer in nitrogen than actively aerated compost (Solano et al. 2001).

Measuring the potentially low and variable flows in a passive aeration system is more challenging than measuring the forced airflow of an active system, especially in experimental or pilot-scale vessels of limited volume. The instrument used must be accurate at low flow rates, introduce very little pressure loss, remain effective and accurate over wide ranges of temperature and humidity, and be amenable to automation so as to effectively track fluctuations in the flow rate. As a research instrument, it should also be inexpensive and robust in laboratory and field environments.

Perhaps because of the aforementioned challenges, there is less published literature about passively aerated composting systems than about actively aerated systems. Fogiel et al. (1999) measured the airflow at the inlet to a compost vessel using a thermal flow meter. Veeken et al. (2002) measured the exhaust flow with a thermal flow meter. Barrington et al. (2003) measured the exhaust flow with an orifice plate. Orifice plates

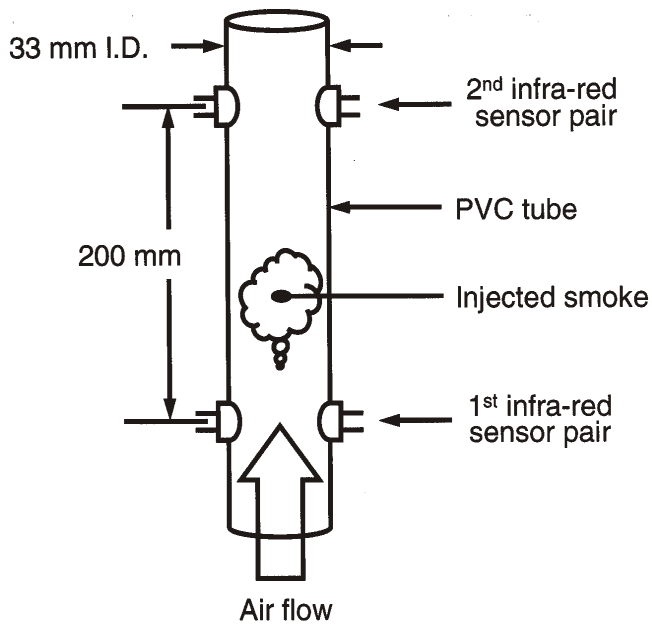


Fig. 1. Schematic of the smoke tracer airflow meter.

and thermal flow meters (or hot-wire anemometers) each have advantages and disadvantages. The orifice plate is the most commonly used flow sensor, but creates a large non-recoverable pressure loss due to turbulence around the plate (Foust et al. 1980). Thermal meters have a low head loss but accurate measurements require knowledge of the temperature, thermal conductivity, and specific heat of the air current. The physical properties of compost exhaust air can vary substantially, since it is often saturated and the temperature can vary from 30 to 70°C, making the measurements taken with a thermal meter difficult to interpret (ASHRAE 2001; Baker 1991). Both types of instrument are more accurate at high flow rates rather than at the low flow rates often encountered in passively aerated composting systems.

The objective of this study was to devise, test, and demonstrate an alternative instrument suitable for measuring airflow in passively aerated compost systems. Several possible methods were considered during preliminary work, including a hot-wire anemometer, a bubble meter, an ultrasonic airflow meter, and a smoke tracer airflow meter. The hotwire anemometer was considered because of its convenience and popularity, but was found to be too unstable at low flow rates. The bubble meter generated too much flow resistance, was difficult to operate, and was potentially difficult to automate. The smoke tracer and ultrasonic meters were therefore chosen for further development and comparison.

## MATERIALS and METHODS

### Smoke tracer meter

Airflow can be measured by injecting a tracer element, such as smoke, into an air stream passing through a uniform conduit (a round pipe in this case) and using sensors to detect its passage at two points along the conduit. From Eqs. 1 and 2, respectively, the apparent air speed and volumetric airflow rate can be calculated from the time interval between the arrival of the smoke at the first and the second detectors, the diameter of the pipe, and the distance between the two sensor pairs. This

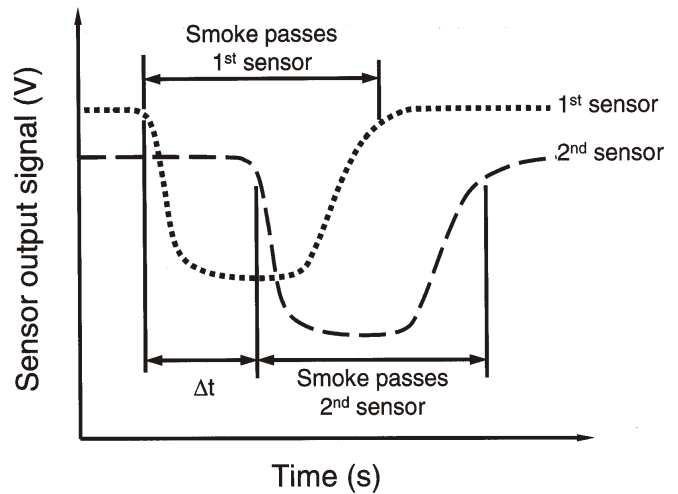


Fig. 2. Theoretical shape of voltage signals from smoke tracer airflow meter.

method causes negligible pressure drop or disturbance of the air stream.

$$v = \frac{L}{\Delta t} \quad (1)$$

$$Q = \frac{\pi}{4} D^2 \frac{L}{\Delta t} = \left( \frac{\pi D^2}{4} L \right) \frac{1}{\Delta t} \quad (2)$$

where:

$v$  = mean air speed (m/s),

$Q$  = volumetric airflow rate (m<sup>3</sup>/s),

$L$  = length of pipe between infra-red transducers (m),

$D$  = diameter of pipe (m), and

$\Delta t$  = time difference between signal drops at two infra-red transducers or times-of-flight between ultrasonic transceivers (s).

In this study, the chosen tracer element was sulphuric acid aerosol generated by a commercially available airflow tester (Flow Check, Draeger Canada Ltd., Mississauga, ON). The white aerosol smoke forms when moist air passes through the tester. The density of the aerosol varies with humidity of the air, but is of approximately neutral buoyancy and is carried in the air stream without influencing the flow pattern. Paired infra-red light-emitting diodes and photodetectors (QED123 and QSD123, Fairchild Semiconductor Corp., South Portland, ME) were installed at two points 200 mm apart in the walls of a 33-mm (inside diameter) polyvinyl chloride (PVC) pipe to detect the passage of the smoke (Figs. 1 and 2). Infrared technology has been widely applied and the transducer pairs are inexpensive and readily available. Smoke was injected into the inlet of the PVC pipe so that it was carried by the air current and passed the detectors sequentially. The smoke blocked the infra-red light beam as it passed between each transducer pair and reduced the output voltage signal from the detector (Fig. 2).

### Ultrasonic meter

A time-of-flight ultrasonic airflow meter was also constructed for use in this study (Brown 1991). A pair of ultrasonic transceivers (QK168, QKits Ltd., Kingston, ON) was installed in a PVC pipe as shown in Fig. 3. Each transceiver can both

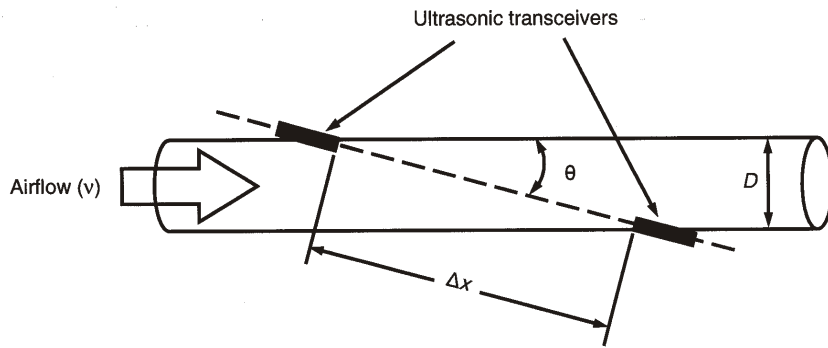


Fig. 3. Schematic of the ultrasonic airflow meter.

send and receive ultrasonic signals. The time for the ultrasonic waves to travel from the upstream transceiver to the downstream one can be calculated using Eq. 3 and the time to travel the reverse path using Eq. 4.

$$t_1 = \frac{\Delta x}{v_s + v \cos \theta} \quad (3)$$

$$t_2 = \frac{\Delta x}{v_s - v \cos \theta} \quad (4)$$

where:

- $t_1$  = time for ultrasonic waves to travel from upstream transceiver to downstream transceiver (s),
- $t_2$  = time for ultrasonic waves to travel from downstream transceiver to upstream transceiver (s),
- $\Delta x$  = direct distance between ultrasonic transceivers (m),
- $v_s$  = speed of sound in air (m/s), and
- $\theta$  = relative angle between ultrasonic beam and mean direction of airflow.

The effect of the air speed is proportional to the time difference between the two flights (Eq. 5), and the corresponding volumetric flow rate can be found using Eq. 6.

$$\begin{aligned} \Delta t = t_2 - t_1 &= \frac{\Delta x}{v_s - v \cos \theta} - \frac{\Delta x}{v_s + v \cos \theta} \\ &= \frac{2\Delta x v \cos \theta}{v_s^2 - v^2 \cos^2 \theta} \approx \frac{2\Delta x v \cos \theta}{v_s^2} \end{aligned} \quad (5)$$

$$Q = \frac{\pi D^2}{4} v = \frac{\pi D^2}{4} \frac{\Delta t v_s^2}{2\Delta x \cos \theta} = \frac{\pi D^2 v_s^2}{8\Delta x \cos \theta} \Delta t \quad (6)$$

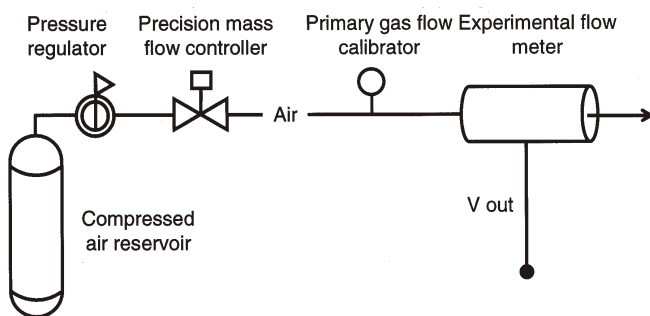


Fig. 4. Schematic of the calibration system.

Since the speed of sound in air is influenced by temperature, the flow meter is sensitive to temperature change. If the temperature of the measured air stream varies substantially, then the speed of sound used in Eqs. 3–6 should be adjusted accordingly (Brown 1991; Reese 2000) by the use of Eq. 7.

$$v_s = 331.5 + 0.60T \quad (7)$$

where:  $T$  = air temperature ( $^{\circ}\text{C}$ ).

Adjustment of the speed of sound was not a concern in this study, where temperature of the inlet air stream measured with the ultrasonic meter in the experiment (about  $15^{\circ}\text{C}$ ) varied by only a few degrees from the calibration temperature (about  $20^{\circ}\text{C}$ ). According to Eq. 7, a  $5^{\circ}\text{C}$  difference in temperature results in error of less than 1%.

### Calibration

The meters were calibrated in the laboratory and the sensitivity of the sensor circuits was adjusted in order to optimize their response. As shown in Fig. 4, compressed lab air (550 kPa) was filtered and warmed to ambient temperature before entering the calibration system. A precision mass flow controller (Mass-Flo<sup>®</sup>, 1179A24CS1BV, MKS Instrument, Wilmington, MA) was controlled by a computer to deliver the airflow (MKS Instruments 2002). A primary gas flow calibrator (DryCal<sup>®</sup>, DCL-H Rev. 1.08, Bios International Corporation, Butler, NJ) was used as the standard to determine the volumetric airflow rate during calibration (Middendorf et al. 2001) and as the basis for the computer control of the air delivery system. The corresponding output signals from the experimental airflow meter were logged automatically. After the data were conditioned offline to determine the measured airflow rates, linear regressions were performed to determine the relationship between the airflow rates measured by the primary gas flow calibrator and the experimental airflow meters (Eqs. 2 and 6). Two independent calibrations of the two meters were conducted and each calibration was performed with duplication. Data from these two independent calibrations were pooled for subsequent regression analysis (Figs. 5 and 6).

### Pressure loss

Pressure loss across a flow meter is influenced by the effective diameter of the flow meter. For steady flow, pressure loss caused by a change in the diameter of a pipe, as in the smoke tracer flow meter, can be estimated with Eq. 8.

$$\Delta P_d = K \frac{v^2}{2\alpha} \quad (8)$$

where:

- $\Delta P_d$  = pressure loss due to change in pipe diameter (Pa),
- $K$  = contraction-loss coefficient (dimensionless), and
- $\alpha$  = flow regime correction factor (dimensionless).

$K = 0.55$  for a large reduction in diameter,  $v$  is the velocity in the conduit of smaller diameter, and  $\alpha = 0.5$  for laminar flow (Geankopolis 1993). The maximum speed recorded in this trial was 0.30 m/s. According to Eq. 8, the pressure loss due to the diameter change from the compost vessel to the smoke tracer flow meter was about 0.06 Pa.

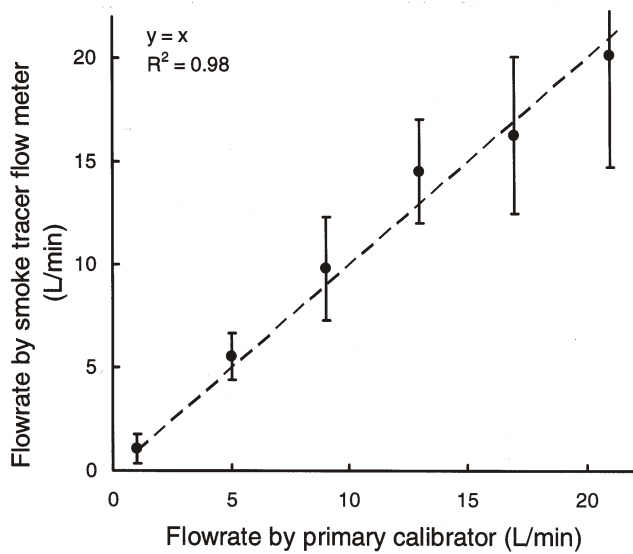


**Fig. 5. Calibration data for the smoke tracer airflow meter. Error bars indicate the standard error (n = 20).**

The pressure drop due to friction losses in the tube of the smoke tracer meter was calculated using the Darcy-Weisbach equation (Eq. 9) and was estimated to be approximately 0.04 Pa (Geankopolis 1993).

$$\Delta P_f = 2f\rho \frac{L}{D} v^2 \quad (9)$$

where:

$\Delta P_f$  = pressure loss due to friction (Pa),  
 $f$  = friction factor (dimensionless), and  
 $\rho$  = density of fluid (kg/m<sup>3</sup>).

Therefore, the total estimated pressure loss across the smoke tracer flow meter was about 0.10 Pa.

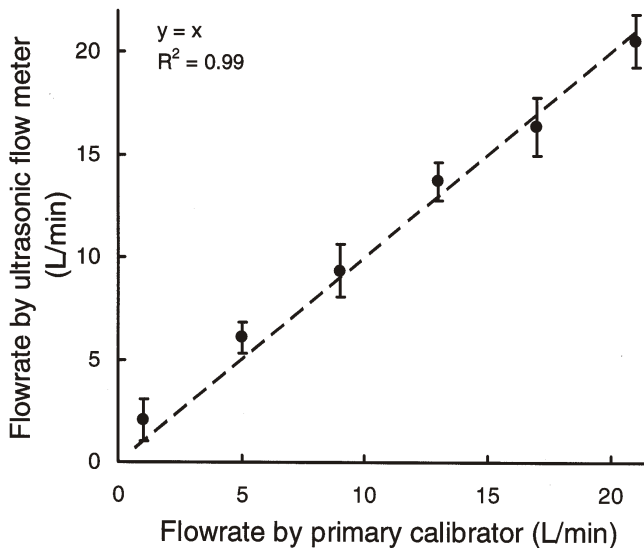


**Fig. 6. Calibration data for the ultrasonic airflow meter. Error bars indicate the standard error (n = 12).**

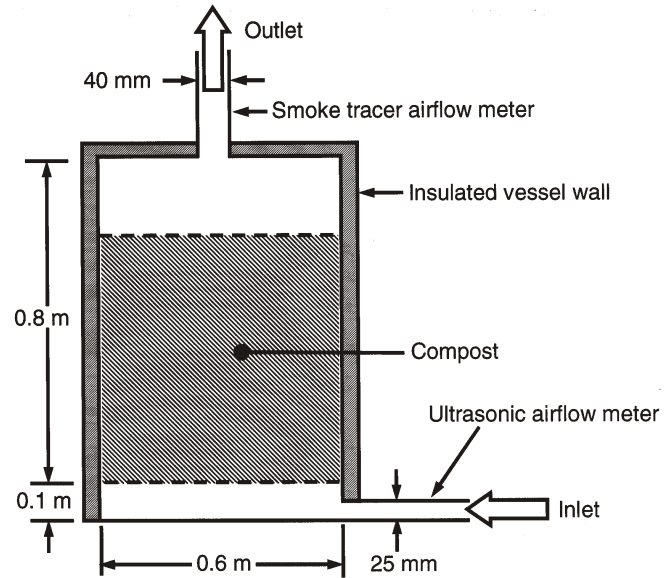


**Fig. 7. Schematic of passively aerated compost vessel.**

The ultrasonic airflow meter was installed in the walls of the existing air inlet pipe and did not appreciably disrupt the airflow, thus causing only negligible pressure loss.

#### Application

Both the smoke tracer and ultrasonic meters were used in a composting trial conducted in a passively aerated, cylindrical, polyethylene vessel, 0.9 m in height and 0.6 m in diameter (Fig. 7). The vessel was insulated and an expanded metal floor was installed 0.10 m from the bottom of the vessel to create an aeration plenum. Fresh dairy manure was mixed with air-dried ground straw, sawdust, and woodchips to obtain a carbon to nitrogen ratio of 35:1 and a free air space of 70%. Carbon and nitrogen content in the substrate were analyzed (Norwest Labs, Edmonton, AB) before and after composting. The initial moisture content of the prepared mixture was 78% (wet basis). At the beginning of the experiment, the depth of the compost in the vessel was 0.50 m. During the trial, the outlet airflow rate was measured using the smoke tracer meter. The performance of ultrasonic devices is inhibited by high relative humidity, so the ultrasonic meter was used to measure the airflow rate only at the inlet.

#### RESULTS and DISCUSSION

The responses of the flow meters were very linear in the calibration range, as indicated by the correlation coefficients ( $R^2$ ) of 0.98 and 0.99 for the smoke tracer and ultrasonic flow meters, respectively (Figs. 5 and 6). Despite its linear response, the measured output voltage from the ultrasonic meter changed very little with increasing flow rate, showing low sensitivity at low airflow rates. The smoke tracer flow meter, for its part, exhibited greater variation at high airflow rates than did the ultrasonic device. The relatively low sampling rate (about 6 Hz), limited by the slow clock speed of the computer used in the trial, was a major contributor to this. At a relatively high airflow rate of 21 L/min, while the average measured flow rate was 20.4 L/min (SD = 5.3 L/min), the mean rounding error caused by the sampling rate would have been 8.3 L/min, or 41% of the

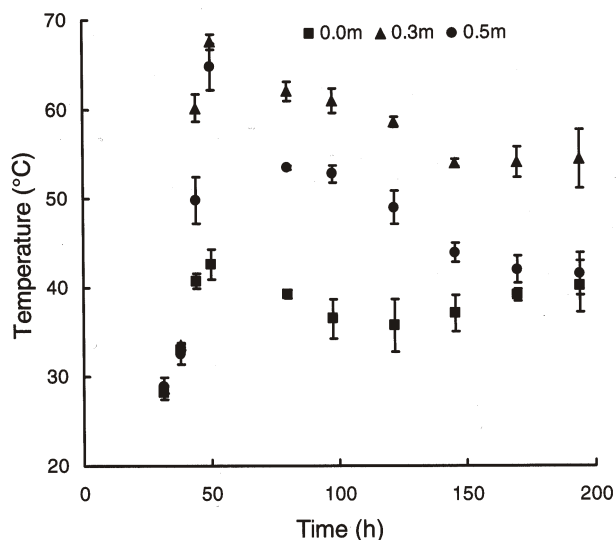


**Fig. 8.** Temperature history at 0, 0.3, and 0.5 m from the bottom of the compost bed. Error bars indicate the standard error ( $n = 2$ ).

flow rate. The mean rounding error in the measurement of the transport time for the aerosol is expected to be one-half of the sampling period, resulting in a systematic overestimate of the transport time and subsequent underestimate of the air flow rate. This source of error is inversely proportional to the sampling frequency, which could easily be greatly increased with current hardware.

The temperature history at different locations in the compost vessel and the flow rate of air through the compost vessel are shown in Figs. 8 and 9, respectively, for the experimental trial. The temperature in the top layer of the compost (0.5 m) followed a typical curve for composting, increasing exponentially to about 65°C during the first 30 h of the trial and then gradually declining to about 40°C over the remaining 150 h. The airflow rate followed the same general pattern (Fig. 8), with a few hours lag time, increasing to a maximum at about 40 h and then gradually declining. This illustrates how buoyancy drove the convective airflow through the vessel as air was warmed by microbial activity in the compost bed.

The vertical temperature gradient illustrated in Fig. 8 was the result of heat and mass transfer processes in the compost. The airflow through the compost was unidirectional, as indicated in Fig. 7, passing through the compost from bottom to top and removing heat, moisture, and other volatile compounds. While heat production during composting is almost completely derived from biological activity (Finstein and Morris 1975), thermal energy is lost mainly as latent heat due to the vaporization of water (VanderGheynst et al. 1997). When the relatively cool, dry ambient air was drawn into the bottom layer of compost (0.0 m), the resultant heat transfer kept the compost there at mesophilic temperatures. Upon reaching the middle layer (0.3 m), the air had already been warmed and moistened and, as a result, biological heat generation during the active composting phase was sufficient to maintain thermophilic temperatures. Upon reaching the top layer (0.5 m), the oxygen content in the airflow had been reduced by microbial activity in the lower layers and carbon dioxide, ammonia, and volatile

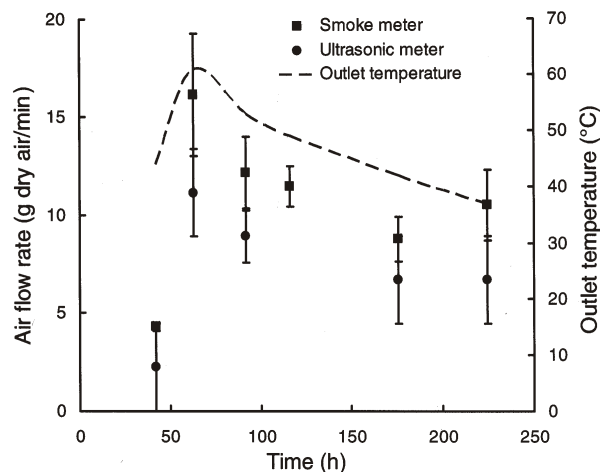


**Fig. 9.** Air flow rate (equivalent mass of dry air) measured at the vessel inlet (ultrasonic meter) and outlet (smoke tracer meter). Dashed line indicates temperature at the top of the compost bed (outlet). Error bars indicate the standard error of two measurements for the ultrasonic flow meter ( $n = 2$ ) and smoke tracer flow meter ( $n = 6$ ).

organic concentrations had been increased. Microbial activity in the substrate was therefore inhibited, while the still unsaturated airflow continued to evaporate moisture from the substrate, shifting heat energy from sensible to latent form and depressing the temperature.

The volumetric and dry mass flow rates at the vessel inlet and exhaust are compared in Table 1. Conversion from volumetric to equivalent dry mass flow rate was done using standard psychrometric relationships, Eqs. 10 and 11 (ASHRAE 2001), based on the assumptions that exhaust air was saturated (100% relative humidity) and that the inlet and exhaust pressures were atmospheric (101.3 kPa).

$$v_a = v_{da} + \mu v_{sa} \quad (10)$$

$$\mu = \frac{\phi}{1 + \frac{(1 - \phi)W_s}{0.62198}} \quad (11)$$

where:

- $v_a$  = specific volume of air ( $\text{m}^3/\text{kg}$  dry air),
- $v_{da}$  = specific volume of dry air ( $\text{m}^3/\text{kg}$  dry air),
- $v_{sa}$  = difference between specific volume of moist air at saturation and that of dry air ( $\text{m}^3/\text{kg}$  dry air),
- $\mu$  = degree of saturation (dimensionless ratio, unity at saturation),
- $\phi$  = relative humidity (%), and
- $W_s$  = humidity ratio at saturation, dimensionless ratio of mass of water vapor to mass of dry air in  $1 \text{ m}^3$  of air.

The average ambient relative humidity in the laboratory was 56.4% (SD = 5.7%) and the average ambient temperature was 23.3°C (SD = 2.2°C). The exhaust flow rate, measured with the smoke tracer flow meter, was consistently higher than the inlet flow rate, measured with the ultrasonic meter. The exhaust flow peaked at about 16 g dry air/min (19 L/min) and then declined to about 9 g dry air/min (9 L/min) by the end of the trial. At the

**Table 1. Airflow rates as measure at the inlet and outlet of the compost vessel.**

Time (h)	Inlet flow rate <sup>†</sup> (ultrasonic flow meter)		Outlet flow rate <sup>‡</sup> (smoke tracer flow meter)			
	Volumetric basis (L/min)	Dry mass basis (g dry air/min) <sup>§</sup>	Volumetric basis (L/min)	Dry mass basis (g dry air/min)	Temperature (°C)	Difference (g dry air/min)
42	1.9 (1.9)	2.2 (2.2)	4.2 (0.2)	4.3 (0.2)	44	2.0
63	9.5 (1.9)	11.1 (2.2)	19.2 (3.7)	16.1 (3.1)	61	5.0
92	7.6 (1.1)	8.9 (1.3)	13.1 (2.0)	12.1 (1.8)	53	3.2
116	n.d. <sup>¶</sup>	n.d.	11.8 (1.1)	11.4 (1.0)	49	n.d.
176	5.7 (1.9)	6.7 (2.2)	8.5 (1.1)	8.8 (1.1)	42	2.1
225	5.7 (1.9)	6.7 (2.2)	9.8 (1.7)	10.5 (1.8)	37	3.8

<sup>†</sup> Mean value with SD in parentheses. Mean air inlet temperature was 23.3 °C and mean relative humidity was 56.4%.

<sup>‡</sup> Mean value with SD in parentheses. Outlet air was assumed to be saturated.

<sup>§</sup> Grams of dry air equivalent per minute

<sup>¶</sup> No data

inlet, the measured flow peaked at about 11 g dry air/min (10 L/min) and then declined to about 7 g dry air/min (6 L/min). According to the stoichiometric analysis described by Haug (1993), more gas is expected in the exhaust since more CO<sub>2</sub> and NH<sub>3</sub> are generated during the oxidation of the substrate and the magnitude of the difference depends on the composition of the substrate and the final composted product (Haug 1993, pp 261-286). Nutrient balances in this study, based on analysis of the compost at the start and end of the trial (Table 2), illustrate the loss of carbon and nitrogen during composting and the potential difference this could make between inlet and exhaust airflow. The data shown are based on the concentrations of two composite samples before and after composting. Comprehensive material balances were not performed since this was beyond the scope of this study.

The smoke tracer flow meter appears to be best suited to laboratory studies of this kind when evaluated according to the criteria stated in the introduction. Unlike the ultrasonic meter, the smoke tracer meter is robust in the face of humidity, temperature, or pressure changes in the air stream. The smoke tracer meter accurately measures small changes in airflow at low flow rates and causes negligible pressure loss, especially if the inside diameter of the body of the flow meter is the same as that of the exhaust duct. In this study, the smoke injection and the determination of the exact time at which the voltage drops occurred at each sensor were done manually, but both of these operations could easily be automated at little cost to increase the accuracy of the measurements. The magnitude of the voltage change from the phototransistor that was used is reduced at

higher temperatures, although the transit time of the tracer smoke is not affected by air temperature. This change in sensitivity could be compensated for by adjusting the value of the variable resistor in series with the phototransistor. A modulated signal might also be used to minimize the effect of temperature change on the sensitivity of the circuit. The accuracy of output of the ultrasonic meter, by contrast, is affected by temperature change, as described previously. The simple components of the smoke tracer flow meter (Fig. 1) made it easy to build and the cost was low compared with that of any available commercial air flow meter. Any general-purpose analogue-to-digital conversion module could be used as a data logging system. The ultrasonic meter, by comparison, requires much more complex components for the ultrasonic transmission and reception and cannot be connected to a computer readily (Becker 2003). To adapt the smoke tracer flow meter for use with piles of compost or windrows, a flux chamber (Frechen et al. 2004) could be employed.

## SUMMARY and CONCLUSIONS

A smoke tracer flow meter was devised to measure airflow through passively aerated compost. Compared with other flow meters used in similar experiments, the smoke tracer flow meter had the advantages of very low pressure loss, low cost, and robust performance under humid conditions. The device was proven in an actual experiment to effectively measure the flow rate of warm, moist exhaust air from passively aerated compost. Further work could be done to completely automate this device. By comparison, an ultrasonic airflow meter had better linear response ( $R^2 = 0.99$ ) but was shown to be poorly suited to this kind of experimental work due to its low sensitivity at low flow rates and high sensitivity to changes in temperature and humidity.

## ACKNOWLEDGEMENTS

This project was financially supported by the Natural Sciences and Engineering Research Council of Canada and the Department of Agricultural, Food, and Nutritional Science of the University of Alberta. The authors thank F. Paradis for reviewing the French translation of the abstract, D. Martineau and I. Ruotsalainen for help with the calibration, and C. Ouellette for help with the electronics.

**Table 2. Total carbon and nitrogen balance per vessel during composting.**

	Initial (g)	Final (g)	Difference (g)	Produced gas <sup>†</sup> (g dry air/min) <sup>‡</sup>
Carbon	3510	2470	1040	1.27
Nitrogen	195	140	55	0.022

<sup>†</sup> Assumed complete conversion of lost C to CO<sub>2</sub> and lost N to NH<sub>3</sub> during high rate stage (50 - 100 h)

<sup>‡</sup> Grams of dry air equivalent per minute

## LIST of SYMBOLS

$D$	diameter of pipe (m)
$f$	friction factor (dimensionless)
$K$	contraction-loss coefficient (dimensionless)
$L$	length of pipe between infra-red transducers (m)
$Q$	volumetric airflow rate (m <sup>3</sup> /s)
$T$	air temperature (°C)
$t_1$	time for ultrasonic waves to travel from upstream transceiver to downstream transceiver (s)
$t_2$	time for ultrasonic waves to travel from downstream transceiver to upstream transceiver (s)
$v$	mean air speed (m/s)
$v_s$	speed of sound in air (m/s)
$\alpha$	flow regime correction factor (dimensionless)
$\Delta P_d$	pressure loss due to change in pipe diameter (Pa)
$\Delta P_f$	pressure loss due to friction (Pa)
$\Delta t$	time difference between signal drops at two infra-red transducers or times-of-flight between ultrasonic transceivers (s)
$\Delta x$	direct distance between ultrasonic transceivers (m)
$\theta$	relative angle between the ultrasonic beam and the mean direction of airflow
$\rho$	density of fluid (kg/m <sup>3</sup> )
$v_a$	specific volume of air (m <sup>3</sup> /kg dry air)
$\phi$	relative humidity (%)
$\mu$	degree of saturation (dimensionless ratio, unity at saturation)
$v_{da}$	specific volume of dry air (m <sup>3</sup> /kg dry air)
$v_{sa}$	difference between specific volume of moist air at saturation and that of dry air (m <sup>3</sup> /kg dry air)
$W_s$	humidity ratio at saturation, dimensionless ratio of mass of water vapor to mass of dry air in a cubic meter of air

## REFERENCES

- ASHRAE. 2001. Psychrometrics. In *Handbook of Fundamentals*, 6.1-6.17. Atlanta, GA: American Society of Heating, Refrigerating and Air-Conditioning Engineers.
- Baker, W.C. 1991. Thermal mass flowmeters and controllers. In *Flow Measurement – Practical Guides for Measurement and Control*, ed. D.W. Spitzer, 335-346. Research Triangle Park, NC: Instrument Society of America.
- Barrington, S., D. Choinière, M. Trigui and W. Knight. 2002. Compost airflow resistance. *Biosystems Engineering* 81(4): 433-441.
- Barrington, S., D. Choinière, M. Trigui and W. Knight. 2003. Compost convective airflow under passive aeration. *Bioresource Technology* 86(3): 259-266.
- Becker, J. 2003. Wind speed meter. *Everyday Practical Electronics* 32(1): 44-51.
- Brown, A.E. 1991. Ultrasonic flowmeters. In *Flow Measurement - Practical Guides for Measurement and Control*, ed. D.W. Spitzer, 415-442. Research Triangle Park, NC: Instrument Society of America.
- Fernandez, L. and M. Sartaj. 1997. Comparative study of static pile composting using natural, forced and passive aeration methods. *Compost Science and Utilization* 5(4): 65-77.
- Finstein, M.S. and M.L. Morris. 1975. Microbiology of municipal solid waste composting. *Advances in Applied Microbiology* 19: 113-151.
- Fogiel, A.C., R.D. von Bernuth, F.C. Michel Jr. and T.L. Loudon. 1999. Experimental verification of the natural convective transfer of air through a dairy manure compost media. ASAE Paper No. 99-4053. St. Joseph, MI: ASABE.
- Foust, A.S., L.A. Wenzel, C.W. Clump, L. Maus and L.B. Andersen. 1980. *Principles of Unit Operations*, 560-562. New York, NY: John Wiley and Sons.
- Frechen, F.B., M. Frey, M. Wett and C. Loser. 2004. Aerodynamic performance of a low-speed wind tunnel. *Water Science & Technology* 50(4): 57-64.
- Geankopolis, C.J. 1993. Design equations for laminar and turbulent flow in pipes. In *Transport Processes and Unit Operations*, 3<sup>rd</sup> edition, 83-100. Englewood Cliffs, NJ: Prentice Hall.
- Haug, R.T. 1993. *The Practical Handbook of Compost Engineering*. Boca Raton, FL: Lewis Publishers.
- Lynch, N.J. and R.S. Cherry. 1995. Design of passively aerated compost piles: Vertical air velocity between the pipes. In *The Science of Composting*, eds. M. De Bertoldi, P. Sequi, B. Lemmes and T. Papi, 973-982. Glasgow, UK: Blackie Academic and Professional.
- Middendorf, P.J., D.L. MacIntosh, L.V. Tow and P.L. Williams. 2001. Performance of electronic flow rate meters used for calibration of air sampling pumps. *American Industrial Hygiene Association Journal* 62(4): 472-476.
- MKS Instruments. 2002. *Bulletin* 1179A-6/02. <http://www.mksinst.com/pdf/1179.pdf> (2005/10/06)
- Reese, R.L. 2000. *University Physics*, 553. Pacific Grove, CA: Brooks/Cole.
- Richard, T.L. 1993. Municipal solid waste composting: Biological processing. *MSW Composting Fact Sheets*, No. 2. Ithaca, NY: Cornell Waste Management Institute.
- Rynk, R. (ed.) 1992. *On-Farm Composting Handbook*. NRAES 54, 24-42. Ithaca, NY: Natural Resource, Agriculture, and Engineering Service.
- Solano, M.L., F. Iriarte, P. Ciria and M.J. Negro. 2001. Performance characteristics of three aeration systems in the composting of sheep manure and straw. *Journal of Agricultural Engineering Research* 79(3): 317-329.
- VanderGheynst, J.S., L.P. Walker and J.Y. Parlange. 1997. Energy transport in a high-solids aerobic degradation process: Mathematical modeling, validation and analysis. *Biotechnology Progress* 13(3): 238-248.
- Veeken, A., V. de Wilde and B. Hamelers. 2002. Passively aerated composting of straw-rich pig manure: Effect of compost bed porosity. *Compost Science and Utilization* 10(2): 114-128.